Design and Stress Analysis of a High Speed Rotor for an Advanced Induction Motor

Matthew T. Caprio, Vasileios Lelos, John D. Herbst
The University of Texas at Austin
Center for Electromechanics
Austin, TX 78712
j.herbst@mail.utexas.edu

Abstract - This paper presents the particular mechanical design considerations and analysis results relating to an induction motor rotor designed specifically for high-speed, power dense, mobile applications. A unique end ring design is presented which balances the mechanical and electrical requirements of the high-speed, high-temperature design. Specification of core lamination material is treated in the context of managing spin stresses and maintaining radial contact pressure over the broad operating speed range. Analysis of the rotor bar extension configuration is described to accommodate the relative growth between the end ring and laminated core at operating speed and temperature. A low temperature joining process for the bar / end ring connections is presented that maintains the strength properties of the age hardened copper alloy materials of the squirrel cage assembly.

I. NAVAL APPLICATIONS OF THIS WORK

The development work presented in this paper was originally targeted toward a compact, power-dense, mobile ground transportation power system application, specifically of the 2 MW, 15,000 rpm, energy storage flywheel motor/generator for a high speed locomotive hybrid electric power system. The locomotive application requirements are however, increasingly relevant to modern naval power system needs, as the goals of the Navy's electric ship program will demand high power density, direct-drive, high-efficiency, low maintenance electric machines for both generation and load driving.

Compact high speed induction machines, such as the one described in this paper, could be immediately useful in naval electric ship applications such as propulsion motors, generators, flywheel energy storage motor/generators and auxiliary drives. Similarly, the developments in high speed rotor design presented in this paper could be applied to other sizes and classes of machines to improve motors in both smaller and larger naval applications.

The analysis and simulation of the motor generator design presented in this paper has been completed, and the machine is currently under fabrication and assembly. Over the next two years, the machine will be tested as an individual component and as part of the hybrid power system, in laboratory ground tests and full performance rolling demonstrations in a locomotive test car. Through these series of tests, the machine electrical and mechanical performance and ratings will be compared to predictions, and validated.

II. MOTOR APPLICATION BACKGROUND

The Advanced Locomotive Propulsion System (ALPS) Project is funded by the Federal Railroad Administration as part of the Next Generation High Speed Rail Program. The goal of the ALPS project is to demonstrate a hybrid electric propulsion system for a high speed passenger locomotive offering performance comparable to electric locomotives without the high cost of route electrification. The propulsion system consists of two major elements: the turboalternator, a high speed generator directly driven by a 5,000 hp gas turbine, and the Flywheel Energy Storage System, an advanced composite flywheel driven by a high speed induction motor/generator [1]. Figure 1 is a simplified block diagram of the propulsion system.

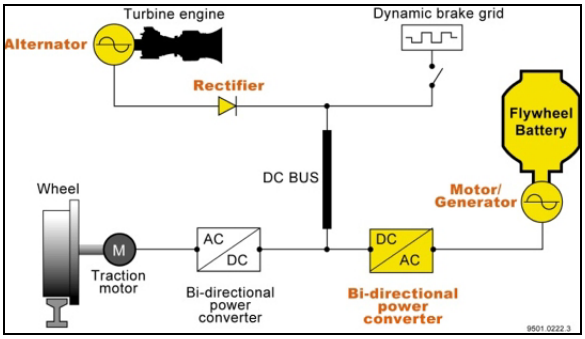

Figure 1. ALPS power system components

The ALPS technologies will be demonstrated in conjunction with an existing Bombardier locomotive; the locomotive's 1,960 V dc bus voltage defines the operating voltage of the motor/generator and power

converter. The ALPS flywheel and motor/generator are designed for 2 MW continuous duty over a speed range from 7,500 to 15,000 rpm. A two pole design was selected for the motor/generator to limit the maximum operating frequency to 250 Hz [2]. Although this results in a somewhat larger and heavier machine than possible with higher pole counts, limiting the operating frequency was an important consideration in the design of the power converter [3]. The 4 kHz switching frequency of the bi-directional power converter provides a high quality 250 Hz waveform to the motor/generator, minimizing harmonics and losses [4].

Power	
Continuous	2.0 MW (2682 hp)
Intermittent	3.0 MW (4023 hp)
Speed Range	7,500 –15,000 rpm
Voltage	1100 V rms L-L
Current	1200 A rms
Efficiency	96.5%
Weight	1900 kg
Overall Length	960 mm
Overall Diameter	813 mm

Table 1. ALPS induction motor ratings

The ALPS induction motor is rated for duty in a dynamic, mobile environment. General mechanical and electrical ratings of the machine can be seen in Table 1. The compact, high speed design is necessary to minimize mass and fit in the available space inside the locomotive tender car. One measure of compactness is "torque per unit rotor volume" or TRV. At the peak torque rating point of 7500 rpm, the ALPS induction machine yields a TRV of 63 kNm/m^3, which is significantly higher than commercially available designs. Perhaps a better measure of this machine's density is "power per unit rotor volume" or PRV, as this takes into consideration the fact that the advanced design can produce high torque at very high speed. At the 2 MW continuous duty power rating, the PRV yields 48780 kW/m^3.

III. HIGH SPEED ROTOR DESIGN

The main components of a conventional induction motor rotor are the shaft, the core (usually constructed of laminated steel punchings), the conductor bars, and the conductive end rings. While this type of construction is relatively simple and robust, for a high speed, high power density application, the centrifugal and thermal stresses are non-trivial and require rigorous design of each of these components.

Figure 2 depicts the topology of the ALPS induction motor rotor, showing the conventional components, as well the spacer, end lamination, and clamping nuts—components specifically developed for this application. The design of these individual components will be described in detail in the following sections.

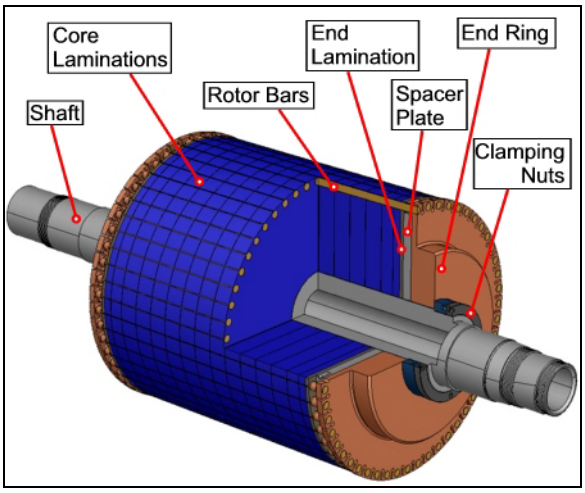

Figure 2. ALPS rotor components

Rotor Core Design: The rotor core proportions of length divided by diameter, or 'L/D ratio', were selected to provide the required torque in the available length envelope, within the bounds of material properties and rotordynamics. The core material mass density and strength properties impose limitations on the maximum surface speed (due to internal spin stresses) and thus play a role in determining the rotor diameter. For this application, the resulting L/D ratio was set to 0.94, with a diameter of 0.364m (14.35 in.) translating into a maximum surface speed, or 'tip speed' of 286 m/s.

Operating a rotor at a rotational speed of 15,000 rpm, with surface speeds in the range of 250-300 m/s reduces the core material selection choices in two ways. The spin stresses alone for a machine operating at this tip speed demand high strength materials, as the hoop loading of the spinning part generates stress levels well in excess of 100 ksi.

In addition to the spin stresses, interference fit preload stresses contribute to the loading of the core material. Operation at high rotational speeds, in excess of about 3600 rpm, requires a high level of balance. For this reason, the rotor core must be concentrically mounted to the shaft throughout the speed range with accuracy. This level of rotordynamic core stability cannot be achieved through the conventional methods of keying or welding the core onto the shaft, but rather only through interference fitting of the core onto the shaft.

Consequently, the required interference fit results in additional stresses in the core material at rest. Further, the net interference pressure at full speed must be sufficient to transmit the machine operating torque.

Conventionally, low coercivity, magnetically "soft," non-oriented silicon electrical steel grades such as the AISI M-15 through M-47 series are employed as laminations in rotor cores. These steel grades are typically chosen due to their low hysteresis loss characteristics incidental to flux cycling of AC machines. However, while their magnetic performance is attractive, the mechanical properties of these steels are inadequate for this high speed application. For example, the published ultimate tensile strength of M-19 steel is 73 ksi [5], whereas this application requires over 110 ksi plus safety margin.

In order to meet the mechanical strength requirements resulting from the tip speed of this design, high-strength aircraft grade AISI 4130 alloy steel was selected for the laminations. Our tests showed that the heat treated, quenched, and tempered laminations achieved a yield strength of 180 ksi, while retaining satisfactory toughness. While there is a compromise in hysteresis losses as the alloy steel has higher coercivity than the "electrical" steels, the increased core losses can be managed through effective cooling. For this application, 29 gauge (0.014 in thick) laminated sheets laser cut and coated with C5 surface insulation were selected to dramatically reduce eddy current losses when compared to solid cores.

The rotor core was designed to be assembled onto the rotor shaft with an interference fit. The interference fit design allows for positive contact between the rotor and shaft throughout the operating speed and temperature range, ensuring stable balance behavior. In addition to maintaining radial contact, sufficient net radial interface pressure must remain in order to transmit torque, with a significant factor of safety for peak transient torques and overspeed.

The analysis of the core interference fit was performed using an axis-symmetric finite element model in Abaqus. The value of the radial interference was optimized for each component through iteration to provide adequate radial contact pressure to transmit torque under full load, hot conditions, without yielding the material in the static cold case. As the torque transmissibility through the interface is dependent on an uncertain coefficient of friction, substantial safety factors must be imposed.

The aggressive level of interference fit selected through the analysis to maintain piloting at full speed is achievable with respect to maximum stresses, but nevertheless presents implementation complexities. When performing fits of this degree, large temperature differential thermal fits are required to install the heated core onto the chilled shaft. Further, when using laminated materials, there is a risk of conical buckling of the core once full interference pressure is achieved during the cool down phase of the thermal assembly.

In general, conical buckling can relax the preload of an interference fit, resulting in excessive rotor growth and axial shifting of the core causing balance problems and insulation faults in wound machines. Although not often reported in the literature, failure of high interference fit laminated rotor core assemblies through conical buckling has occurred in prototype machine designs, including one at our research laboratory.

For the ALPS rotor, a novel design methodology was devised to predict and prevent conical buckling of the core through structural design. This approach depends on the axial deflection stiffness of specifically designed features of the rotor structure to contain the buckling motion.

The buckling prevention analysis consists of approximating the force-deflection characteristics of individual buckled laminations, and applying those forces to a finite element model of the structure to quantify the resulting deflection. A buckling force-displacement curve was generated based on closed form predictions for a single lamination, and is shown in Figure 3.

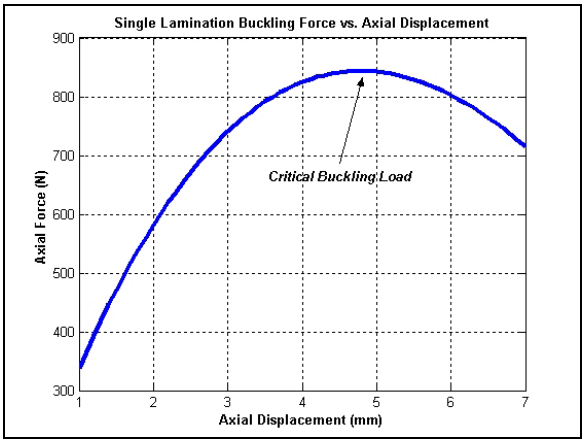

Figure 3. Predicted force of buckling lamination

As the predicted axial forces generated by the buckling lamination increase to a peak value with increasing displacement and then roll off, a peak buckling force can be estimated, and its respective deflection level is defined as the "*critical buckling deflection*." The peak load is then applied to the structural model, and the resulting deflection is measured. The analysis criterion assumes that if the axial displacement of the rotor structure is equal to or

greater than the critical buckling deflection, the core will conically buckle. If however the resulting displacement is substantially less than the critical buckling deflection, the assembly is presumed to be structurally stable, with only negligible amount of conical deformation of the core during assembly.

For the ALPS rotor, the bolstering features incorporated into the rotor structure to prevent buckling include the end lamination, the balance ring spacer, the thick section end ring inner diameter, and the clamping nuts. Buckling analysis showed that the assembly deflection due to peak buckling loads is only a small fraction of the critical buckling deflection, indicating that the design is stable against conical buckling. In addition to this integral structure, a stiff core clamping fixture is used during the assembly and removed after the core cools to room temperature.

This design and analysis approach to preventing conical buckling of high interference laminated rotor cores was successfully demonstrated with the recent fit of the core of another machine in our laboratory, without buckling.

Conductor Bar Design: Squirrel cage induction rotors can be manufactured in two ways: cast, or "fabricated". Cast rotors are conventionally built with integral bars and end rings, formed directly in the lamination stack, with shot-poured aluminum. The cast design is economical for mass production, but as will be shown in a later section, the aluminum materials are insufficient to handle the spin stresses for the end ring in this application. Recent developments have proven that rotors can be successfully cast with copper for higher efficiency [6], however, to date these rotors have been limited to copper grades with low strengths.

A fabricated rotor cage is therefore the only option in this high speed application given the strength levels required from the end ring and bar materials. With this fabrication approach, bars are individually machined, inserted into the core holes, and joined to the end rings.

It is common for motors operating from fixed frequency line voltage to have rectangular section deep bars in order to achieve good starting characteristics at zero speed [7]. However, as this application is driven by a variable frequency power converter with vector control, high torque is available throughout the speed range without the need for non-uniform cross section bars. This fact allows the design to incorporate round cross section rotor bars which are easier to manufacture, assemble, and provide reduced contact stress on the core lamination teeth.

At the tip speed of this application, the dead weight radial loading of the rotor bars bearing on the lamination slot teeth is substantial. As shown in Figure 4 (deformation exaggerated), the high stresses from these radial loads are apparent in both the bars and on the teeth of the laminations which restrain them. The round cross section bars minimize both the contact stresses in the copper material and the peak loading on the steel core teeth, providing an excellent geometry for high speed applications.

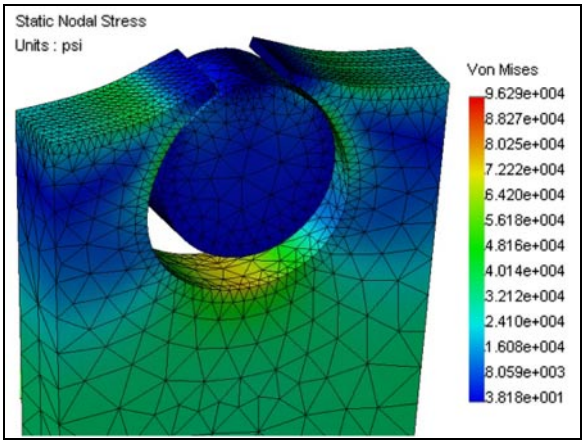

Figure 4. Round bar geometry minimizes stress

Selection of the rotor bar material required a balance between mechanical strength properties and electrical resistance. In order to withstand the bearing loading of the high spin stresses and the stress concentration at the area exiting the rotor core, higher strength copper alloys were investigated. Age hardened Zirconium Copper (CDA # C15000) was selected for its combination of high strength (>60 ksi ultimate strength) and high electrical conductivity (90% IACS). In addition to having higher strength than traditional oxygen free copper (OFC), the ZrCu also better maintains high strength through high temperature exposure—important in this power dense application [8].

End Ring Design: The end ring, or "end connector," is the component of a squirrel cage induction machine that completes the electrical circuit between the individual rotor bars. Conventionally, the end ring is not connected to the shaft, but rather supported by the rotor bars themselves. For this high speed application, the end ring must instead be self supporting, as the bars can not provide enough stiffness to maintain accurate centering and balance of the end ring under the high loading of rotating imbalance.

The high speed of the ALPS motor therefore demands an advanced end ring design that is concentrically piloted on the shaft. Thermally

induced stresses add further complexity to the end ring design in this application. The high power density of the ALPS machine implies that the operating temperatures of the rotor are relatively high, even with forced air cooling. The temperature growth of the rotor, constructed of dissimilar metals with large differences in thermal expansion coefficients, results in high stresses at the end ring. This phenomenon is well recognized during line starting of industrial induction motors [9].

Intelligent material selection, feature design, and analysis were required for the successful design of the advanced end ring of the ALPS motor. Conventional aluminums or OFHC coppers have insufficient strength to withstand the spin stresses and shaft interference fit required for high speed, stable balance operation. Beryllium copper (CDA # C17510) with a tensile strength >100 ksi and conductivity >60% IACS was selected for the end ring in order to withstand the stresses and provide sufficiently low electrical resistance.

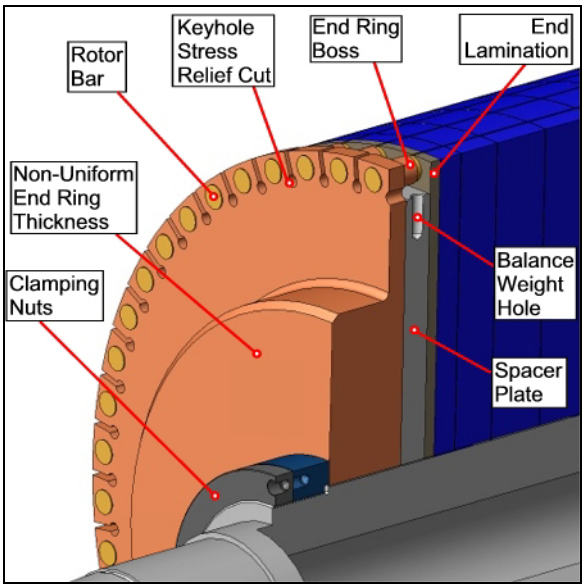

Figure 5. Unique end ring design features

Unique design features were incorporated into the end ring to manage the high spin and thermal growth stresses, as shown in Figure 5. A non-uniform cross section design with an axially thick inner diameter and thin outer diameter allow the end ring to be self supporting with an interference fit to the shaft, while providing axial compliance to allow for thermal bar growth (patent application in progress). A keyhole stress relief feature (patent application in progress) in the outer diameter of the end ring isolates the solder joint area from the centrifugal hoop stresses. The spacer plate provides a region for the relative radial growth difference the end ring and core to be absorbed in bending of the bar rather than shear. The circular boss feature (patent application in progress) surrounding the bar hole of the end ring serves to blend the deflections and reduce stress concentrations in the area of the bar joint.

Electrical FEA was performed using QuickField to verify that the thick section inner diameter of the end ring is effectively used by carrying significant current levels. Due to the two-pole design of the motor, the current path through the end ring is radial, across the diameter. As shown in a plot of the Joule heating losses in Figure 6, the current flow does in fact crowd the inner diameter of the end ring. The thick inner diameter section of the end ring is therefore valuable in reducing the total resistance and I^2R losses of the circuit, in addition to providing the mechanical role of supporting the spin loading.

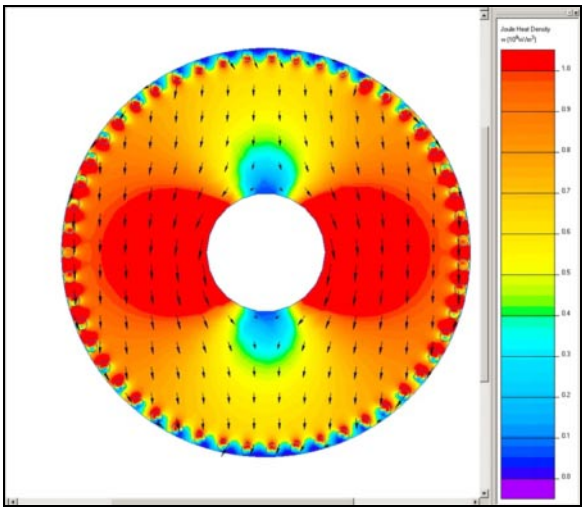

Figure 6. Joule heating concentration in end ring

The analysis of the end ring and bar connection area including the soldered joint was performed using a 3D finite element model with CosmosWorks. Analyzing the true geometry in this area is critical as the interplay of rotating forces and thermal growth results in complex deflection modes that can not be accurately approximated. Thermal analysis was first performed using detailed loss estimates for each rotor component from the EM design code outputs. Convection coefficients and bulk fluid boundary conditions were computed through a heat balance algorithm and MacroFlow CFD cooling air velocity estimates. Figure 7 shows the steady state temperature distribution in the rotor for full load operation in a worst case 50°C ambient environment.

The thermal distribution mesh was imported into the structural analysis model, and the combined thermal-mechanical loading at 15,400 rpm overspeed was analyzed for stresses and displacements. The

resulting compound deflection mode of the end ring and bars (shown exaggerated in Figure 8) generates significant stresses in the joint area.

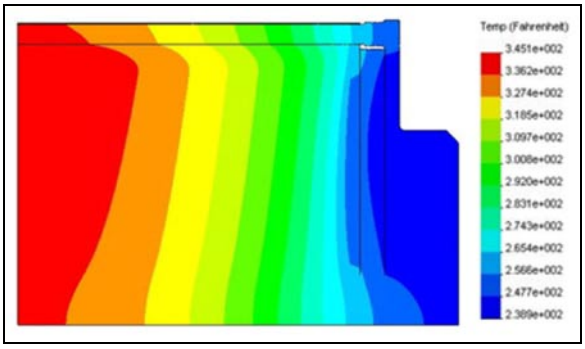

Figure 7. Steady state rotor operating temperatures

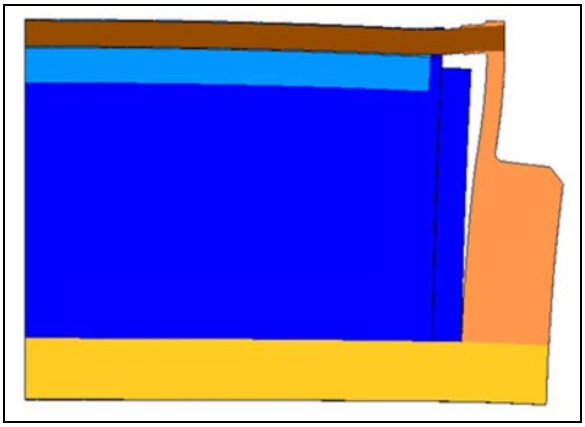
Figure 8. Deflection mode due to thermal and spin

The end ring boss feature graduates the stiffness of the bar's support, thereby reducing the reaction contact and redistributes shear stress concentrations to manageable levels. Whereas peak shear stresses at the sharp corner without the boss feature were approximately 24 ksi, the introduction of the boss dramatically reduced the predictions to less than 9 ksi, as shown in Figure 9.

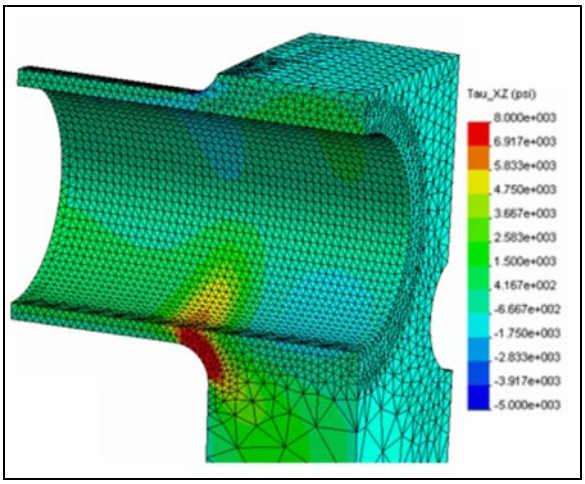

Figure 9. Shear stresses in solder joint area

The deflected shape of the bar due to the relative growth differential between end ring and the core resulted in high stresses on laminations at the end of the core. Therefore, a thicker end lamination plate was installed at each end of the lamination core to manage the concentrated stresses. To address this localized stress, we selected AISI 4340 steel with a 195-210 ksi yield strength for the end laminations.

Spacer and Balance Ring Design: The spacer component was incorporated into the design in order to reduce the shear stresses on the bar joint by providing a region to redistribute the relative growth between the end ring and core. However, the spacer serves double duty as an integral balance ring.

The spacer plate is equipped with radial threaded holes for trim balance weights. The weights are inserted radially, accessed between the rotor bars. The trim balance capacity of the ring is governed by the diameter and depth of the holes, and the maximum density of the weights.

The imbalance correction capacity of the balance ring was determined based on the maximum amount of mass center error that is tolerable through the assembly procedure. Coarse balancing of the rotor is accomplished by offset grinding of the shaft bearing journals. This process is accurate within 0.001" of mass center offset. The balance ring hole pattern is thus designed to provide the inertial characteristics of more than 0.001" of rotor mass center imbalance. Balance will be corrected to within 0.0001" of mass center offset for high speed operation.

Material selection for the spacer component depended on the electromagnetic conditions in that area. As this component is adjacent to the core, in the fringe regions of the machine's flux path, non-ferrous material is needed to avoid increased hysteresis losses, and unnecessary end ring leakage inductance. Additionally, the spacer must be mechanically self supporting through its interference fit at the shaft, consequently, it must possess high strength. For these reasons, Inconel 718, a low permeability nickel alloy was chosen for the spacer.

Shaft Design: The shaft of the ALPS motor is constructed of quenched and tempered 4142 alloy steel, selected for its combination of high strength and toughness. Heavy wall tubing stock was specified as the shaft is hollow. The hollow shaft is advantageous for two purposes: it reduces the stresses in the core at the interference fit, and effectively stiffens the rotor, raising the bending modes of the rotor, improving the rotor dynamics.

The hollow shaft reduces the stresses in the core laminations in the area of the interference fit by adding compliance to the assembly. The hollow shaft, being more compliant than a solid shaft, shares a portion of the total displacement preload necessary for the interference fit. In this way, the amount of displacement absorbed by the laminations alone is reduced, thereby reducing the preload stresses.

Another advantage of the hollow shaft is improved rotordynamic performance. The broad operating speed range and high upper speed of this machine directly coupled to the flywheel, demand minimal vibratory response. Appropriately designed inertial properties selected through the core L/D ratio are primary to good rotordynamic response, and the hollow shaft further improves the performance. By removing the center of the shaft, significant mass is removed, with very little reduction in shaft stiffness. The net result is an effectively stiffer rotor, which assists in driving the first bending mode safely out of the machine's operating speed range.

Due to gyroscopic stiffening, the frequency of the vibratory modes of the ALPS rotor change with speed. The natural frequencies of the system were analyzed and identified with XLRotor, a rotordynamics spreadsheet program. The forward rigid body critical speeds must be traversed on the way to the 7,500-15,000 rpm flywheel operating speed range. As shown in Figure 10, the conical mode intersects the 20% margin surrounding the synchronous excitation line near 7,500 rpm. The response of the conical mode is minimized to acceptable levels by damping included in the system by squeeze film dampers which house the rotor bearings. The first bending mode intersects the 20% margin on synchronous excitation at approximately 27,000 rpm, well above the maximum operating speed of 15,000 rpm.

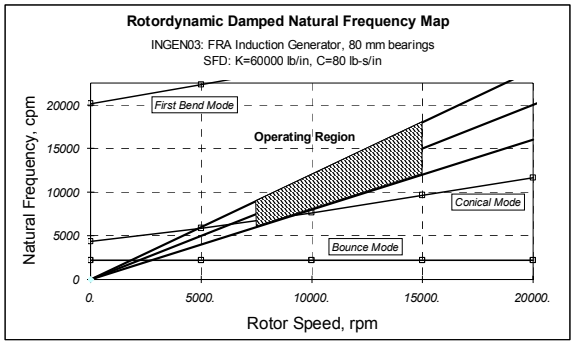

Figure 10. Critical speed map of the ALPS rotor

The ALPS rotor shaft is directly connected to the flywheel shaft through a flexible coupling. The flexible coupling fits to the rotor shaft via a spline. As the diameter of the shaft was minimized to maximize bearing life (by reducing the dN operating speed of the bearings), very little cross sectional shaft area is available for transmitting torque through the spline. In order to achieve satisfactory stress levels in the spline, additional material was preserved at the inner diameter of the shaft in the region of the spline by trepanning the shaft tubing to two sizes: a larger inner diameter for a majority of the shaft length underneath the interference fits, and a smaller inner diameter at the splined drive end.

IV. MOTOR MANUFACTURING

Solder Processing Development: The rotor bars must be joined to the end rings for electrical and mechanical purposes with sound, consistent, reliable joints. The strength requirements for the end ring-to-bar joint were determined through the coupled thermal-stress analysis. Preserving the material properties of the age hardened copper alloys imposes thermal profile limits on the selected joining process. Conventional brazing techniques will not meet these specific requirements, therefore a customized low temperature, high-strength solder joint is engineered for this application.

The targeted strengths of the solder joint, based on the peak tensile and shear stress components identified in the FEA model results with appropriate margin, are 25 ksi and 15 ksi respectively. Brush-Wellman, the supplier of the end ring BeCu material recommends specific alloys for brazing the BeCu alloys which easily meet these strength levels, such as BAg-1, BAg-8, and RBCuZn-D [10]. However, the process temperatures of these joining fillers exceed the age hardening temperature range (450-550°C) of both the BeCu and the ZrCu, and in some cases the solution annealing temperature (900°C) as well. The process of brazing with these fillers would therefore dramatically reduce the mechanical strength of the end ring and bar to unacceptable levels. Re-heat treating of the copper alloys after brazing is not possible as these components are then part of a larger, multiple material assembly.

A number of Au, In, and Zn based filler metals with low process temperatures (less than 450°C) have been successfully used in other applications, demonstrating high strength. For example, the eutectic 80Au-20Sn solder has a solidus temperature of 280°C and rated tensile strength of 40 ksi [11], and is used extensively in the field of microelectronics packaging [12] where high operating temperatures induce large thermal stresses. Other alloys such as Au-12Ge and Au-18In have demonstrated both tensile and shear yield strengths above 20 ksi in similar applications [13].

Testing and process development of low temperature, high strength soldering methods is currently underway. Developments in this area are focused on proper surface preparation and oxidation-shielding platings and fluxes to adapt the specialized Au based filler metals to the base metals in this motor joint application. Heating methods, including torch, resistance, and induction are being investigated to consistently provide the necessary localized heating. Furnace processing of the rotor is not desirable due to the temperature sensitivity of the numerous coatings, insulative films, and bonding agents in the rotor core.

Status: Manufacturing and fabrication of the ALPS induction motor components and assemblies is currently underway at the time of this writing. Initial laboratory testing of the completed motor is scheduled for late 3rd quarter of 2004, followed by static full ALPS power system testing in the 2nd quarter of 2005. The power system will then be integrated into the locomotive test cars and demonstrated on a test track in the 3rd and 4th quarters of 2005.

V. CONCLUSIONS

The 2 MW ALPS flywheel induction motor-generator employs an advanced rotor design that enables high speed operation in a compact package. Novel end ring features such as the keyhole stress relief and the bar hole boss extension reduce stresses on the solder joint area to permit low temperature joining that preserves the mechanical properties of the heat treated copper alloys. The advanced motor design provides high performance for ground transportation that could be readily extended to suit demanding naval applications.

VI. REFERENCES

[1] J.D. Herbst, M.T. Caprio, R.F. Thelen, *Status of the Advanced Locomotive Propulsion System (ALPS) Project*, 2003 ASME International Mechanical Engineering Congress & Exposition (IMECE '03), November 16-21, 2003, Washington D.C.

[2] J.D. Herbst, M.T. Caprio, R.F. Thelen, *2 MW 130 kWh Flywheel Energy Storage System*, Electrical Energy Storage – Applications and Technology (EESAT2003), October 27-29, 2003, San Francisco, CA.

[3] R.F. Thelen, J.D. Herbst, M.T. Caprio, *A 2MW Flywheel for Hybrid Locomotive Power*, IEEE Semiannual Vehicular Technology Conference, October 6-9, 2003, Orlando, FL.

[4] R.F. Thelen, *Specification and Design of a 2MW, 250 Hz Motor Drive for FESS Service*, Proceedings of the Electricity Storage Association, Annual Meeting 2002, Milwaukee, WI, October 9-11, 2002.

[5] *Selection of Electrical Steels for Magnetic Cores*, Armco Electrical Steel Products, Butler, PA, 1985.

[6] J.G. Cowie, *The Die-Cast Copper Motor Rotor is a Commercial Reality*, Update: Copper Motor Rotor, Volume 3, Issue 3, June 2003, Copper Development Association Inc., New York, NY.

[7] A.E. Fitzgerald, C. Kingsley, S.D. Umans, *Electric Machinery, 5th Ed.*, p. 359, McGraw-Hill, 1990.

[8] *Amzirc Technical Data*, American Metal Climax Inc., New York, NY, 1966.

[9] M. Hodowanec, W. R. Finley, *Copper versus Aluminum Induction-Motor Rotors: Which Construction is Best?*, IEEE Industry Applications Magazine, July/August 2002.

[10] *Tech Briefs: Brazing Copper Beryllium*, Brush Wellman Inc., Cleveland, OH, 1985.

[11] *Product Data Sheet: Solder Wire*, Indium Corporation of America, Utica, NY, 1997.

[12] C. Kallmayer, H. Oppermann, G. Engelmann, E. Zakel, H. Reichl, *Self-Aligning Flip-Chip Assembly using Eutectic Gold/Tin Solder in Different Atmospheres*, IEEE/CPMT International Electronics Manufacturing Technology Symposium, Austin, TX, 1996.

[13] F.M. Hosking, J.J. Stephens, J.A. Rejent, *Intermediate Temperature Joining of Dissimilar Metals*, AWS Welding Journal, Welding Research Supplement, April 1999.

VII. ACKNOWLEDGEMENTS

This material is based upon work supported by the USDOT Federal Railroad Administration cooperative agreement, DTFR53-99-H-00006 Modification 4, dated April 30, 2003. Any opinions, findings, and conclusions or recommendations expressed in this publication are those of the authors and do not necessarily reflect the view of the Federal Railroad Administration and/or U.S. DOT.